DEVELOPMENT OF COCCOLITHOPHORE-BASED TRANSFER FUNCTIONS IN THE WESTERN MEDITERRANEAN SEA: A SEA SURFACE SALINITY RECONSTRUCTION FOR THE LAST 15.5 KYR

B. Ausín[a] (b_ausin@usal.es); I. Hernández-Almeida[b] (ivan.hernandez@giub.unibe.ch); J-A. Flores[a] (flores@usal.es); F-J. Sierro[a] (sierro@usal.es); M. Grosjean[b] (martin.grosjean@oeschger.unibe.ch); G. Francés[c] (gfrances@uvigo.es); B. Alonso[d] (belen@icm.csic.es).

[a]Department of Geology, University of Salamanca, Plaza de los Caídos s/n, 37008 Salamanca, Spain

[b]Institute of Geography and Oeschger Centre for Climate Change Research, University of Bern, Erlachstrasse 9a, 3012 Bern, CH-3012 Bern, Switzerland.

[c]Department of Marine Geosciences, University of Vigo, Campus As Lagoas – Marcosende, 36310 Vigo, Spain.

[d]Department of Marine Geosciences, Instituto de Ciencias del Mar (CSIC), Passeig Marítim de la Barceloneta, 37-49. E-08003 Barcelona, Spain.

Correspondence to:

Blanca Ausín (b_ausin@usal.es)

Plaza de los Caídos s/n, 37008 Salamanca, Spain.
Tel: (+34) 923 294497
Fax: (+34) 923 294514

Abstract

A new dataset of 88 marine surface sediment samples and related oceanic environmental variables (temperature, salinity, chlorophyll-*a*, oxygen, etc.) was studied to quantify the relationship between assemblages of coccolithophore species and modern environmental conditions in the Western Mediterranean Sea and the Atlantic Ocean, west of the Strait of Gibraltar. Multivariate statistical analyses revealed that coccolithophore species were primarily related to sea surface salinity (SSS), explaining an independent and significant proportion of variance in the coccolithophore data. A quantitative coccolithophore-based transfer function to estimate SSS was developed using the Modern Analog Technique (MAT) and weighted-averaging partial-least square regression (WA-PLS). The bootstrapped regression coefficient (R^2_{boot}) was 0.85_{MAT} and $0.80_{WA\text{-}PLS}$, with root-mean square error of prediction (RMSEP) of 0.29_{MAT} and $0.30_{WA\text{-}PLS}$ (psu). The resulting transfer function was applied to fossil coccolithophore assemblages in the highly resolved (~65 yr) sediment core CEUTA10PC08 from the Alboran Sea (Western Mediterranean) in order to reconstruct SSS for the last 25 kyr. The reliability of the reconstruction was evaluated by assessing the degree of similarity between fossil and modern coccolithophore assemblage, and comparison of reconstruction with fossil ordination scores. Analogs were poor for the stadials associated with Heinrich Event 2 and 1 and part of the Last Glacial Maximum. Good analogs indicate more reliable reconstruction of the SSS for the last 15.5 kyr. During this period, several millennial and centennial SSS changes were observed and associated with sea-level oscillations and variations in the Atlantic Water entering the Alboran.

Key words: transfer function; coccolithophores; salinity; Western Mediterranean Sea; Atlantic Ocean; Last Glacial Maximum.

1. INTRODUCTION

Coccolithophores are one of the major components of marine phytoplankton. They are sensitive to changes in many environmental variables, such as nutrients, temperature and salinity and are widely used in qualitative paleoenvironmental studies (Baumann et al., 2005; Guerreiro et al., 2013; Guerreiro et al., 2014). These studies provide general insight into the response of coccolithophores to environmental variables, but quantitative studies (e.g. transfer functions) allow assessing these relationships in a more rigorous and clear manner. Transfer functions are based on the calibration of the modern relationship between organisms and environmental conditions, and this information is in turn used to reconstruct past environmental variables. Different statistical approaches based on coccolithophores have been proposed in order to generate quantitative paleoreconstructions of different ecological variables. Giraudeau and Rogers (1994) used factor analyses and multiple regressions to estimate chlorophyll-*a* from

coccolithophore census counts in surface sediment samples in the Benguela upwelling area. Several authors (Beaufort et al., 2001, 1997; Incarbona et al., 2008) calibrated the relative abundance of the coccolithophore *Floriphaera profunda* in surface sediment samples with respect to primary productivity and reconstructed past variations of this parameter in the Indian and Pacific oceans and in the Central Mediterranean Sea. Saavedra-Pellitero et al. (2011, 2013) used linear regression methods to derive past SST estimates in the southeast Pacific Ocean from coccolithophore census counts and accumulation rates. Bollmann et al. (2009) and Bollmann and Herrle (2007) applied multiple linear regressions to morphometric measurements of the coccolithophore *Emiliania huxleyi* from globally distributed core-top and plankton samples to obtain modern and past sea surface salinity (SSS) estimates.

To date, no coccolithophore-based transfer function has been applied in the Western Mediterranean Sea, a semi-enclosed basin situated at mid-latitudes (Fig. 1a). In this region evaporation exceeds precipitation plus runoff, such that water budgets tend to be balanced by the advection of relatively less saline Atlantic Water (AW) through the Strait of Gibraltar (Bèthoux, 1979). The AW flows eastward while mixing with Mediterranean water to form the Modified Atlantic Water (MAW) at the surface (100-200 m) (Millot, 1999). This distinctive feature affects the spatial distribution of some environmental parameters such as SST and SSS, leading to the development of well-defined longitudinal gradients between the Atlantic Ocean and the Western Mediterranean in annual terms. In this confined basin, the estimation of changes in those environmental parameters is essential for determining Atlantic-Mediterranean water mass exchange through the Strait of Gibraltar in the past (Rohling and Bigg, 1998; Schmidt, 1998). This exchange depends on variations in the hydrological cycle, ice-volume effects, and Mediterranean circulation patterns, which have a thermohaline origin (MEDOCGROUP, 1970).

The aim of this study is to explore the potential of coccolithophores for the development of quantitative reconstructions in the Western Mediterranean Sea. We study the response of coccolithophore assemblages from surface sediment samples from Atlantic Ocean and Mediterranean Sea to environmental variables. The resulting calibration model (transfer function) for salinity was used to reconstruct SSS changes at high-resolution in the Alboran Sea (Fig. 1a) for the last 25 kyr. The reliability of the reconstruction was assessed by analysis of the similarity between fossil and modern coccolithophore assemblages, and fossil ordination scores. Finally, centennial and millennial SSS changes are described and discussed, and compared with regional records of SST and organic matter preservation.

2. MATERIALS AND METHODS

2.1. Modern training set

69 *2.1.1. Surface sediment samples*

70 Initially, 117 core tops located around a horizontal transect along the Western Mediterranean
71 Sea and near the Gulf of Cadiz in the Atlantic Ocean were selected. They had been retrieved at
72 varying water depths ranging from 70 to 2620 m during several oceanographic surveys and
73 were stored at the University of Vigo and at the Core Repository of the Institute of Marine
74 Sciences- CSIC in Barcelona. The first cm (or the second, if the first was unavailable) of the
75 117 core tops was sampled, assuming that it essentially represents present-day conditions.

76 *2.1.2. Environmental variables*

77 Data on temperature (Locarnini et al., 2013), salinity (Zweng et al., 2013), chlorophyll-*a*
78 (Boyer et al., 2013), oxygen content and saturation (García et al., 2014a), nitrate, phosphate, and
79 silicate (García et al., 2014b) were obtained from the 2013 World Ocean Atlas (WOA13), and
80 mixed layer depth (Monterey and Levitus, 1997), total alkalinity (T_{ALK}) and total dissolved
81 inorganic carbon (DIC) (Goyet et al., 2000) for the training set sites were taken for a grid of 1º
82 longitude by 1º latitude, using weighted averaged gridding by Ocean Data View (ODV)
83 software (Schlitzer, 2014). Similarly, data on pH and carbonate (CO_3^{2-}) were calculated using
84 the 'derived variable' tool of ODV software. These data have been averaged annually and
85 seasonally (for summer and winter) from 1955 to 2012 and were selected at 10, 20, 30, 50, 75,
86 100, 125, 150, and 200 meters water depth.

87 **2.2. Fossil data set**

88 The fossil coccolithophore data set used for the reconstruction comprises coccolithophore
89 census counts from core CEUTA10PC08 (36°1′22″N, 4°52′3″W; 914 mbsl), located in the
90 Alboran Sea, previously published by Ausín et al. (2015). Fossil assemblages show a good-to-
91 moderate degree of preservation. Location of this core lies under the modern path of the AW at
92 the surface, near the Strait of Gibraltar (Fig. 1a). Sediment core chronostratigraphy was based
93 on 15 radiocarbon ages and covered the time span from 25 to 4.5 ka calibrated BP at a ~65 yr
94 temporal resolution (Ausín et al., 2015). All dates reported in this study are given in calibrated
95 ages BP.

96 **2.3. Micropaleontological analyses**

97 Both modern (surface sediment) and fossil (downcore) samples were prepared for
98 coccolithophore analyses according to the techniques proposed by Flores and Sierro (1997). A
99 polarized-light microscope at 1000x magnification was employed to identify and count at least
100 500 coccoliths in each sample, belonging to 21 different taxa. Species whose relative abundance
101 was < 1 % in the first count were considered later in 20 visual fields in order to estimate their
102 abundance accurately. The final relative abundance of each species in each sample was then

recalculated. *Gephyrocapsa* specimens smaller than 3 µm were lumped together and designated "small *Gephyrocapsa"* (Flores et al., 1997). The "medium *Gephyrocapsa*" group was made up of *Gephyrocapsa* whose size was between 3 and 5 µm. Two sizes of morphotypes of *E. huxleyi* (< 4 µm and > 4 µm) were considered owing to their different ecological and biostratigraphic significance in the study area. Similarly, *G. oceanica* was split according to a size criterion of < 5 and > 5 µm owing to their comparable potential ecological significance. Other taxa identified in this study were *Calcidiscus leptoporus*, *F. profunda, Gephyrocapsa* cf. *caribbeanica, Gephyrocapsa muellerae*, *Helicosphaera* spp.*,* and *Syracosphaera* spp. (as dominant taxa). The rare taxa identified were *Braarudosphaera bigelowii, Calciosolenia* spp.*, Coccolithus pelagicus* subsp. *braarudii, Coccolithus pelagicus* subsp. *pelagicus, Oolithotus fragilis, Pontosphaera* spp*., Rhabdosphaera clavigera, Umbilicosphaera* spp. and *Umbellosphaera* spp.

Twenty-nine samples were finally eliminated from the initial modern data set owing to their high content (> 10 %) in obviously reworked nannofossils. These taxa belong to older stratigraphic levels (consistently older than the Pliocene in this study), meaning that they were resuspended and transported from their original location to the sample site, and they lack any relationship with modern environmental conditions. 10 % of reworked specimens was chosen as an acceptable threshold below which the sample could be retained in the modern training set, after ruling out these reworked specimens, without compromising the statistical representativeness of the major species (Fatela and Taborda, 2002). Later examination of the spatial distribution of reworked specimens in the retained samples revealed that those with the highest percentages were close to river mouths, relating reworked specimens to river discharges and suggesting that the rest of the assemblage could be considered autochthonous. Thus, the final training set (supplementary material) comprised 88 surface samples (Fig. 1b): 78 from the Western Mediterranean (58 from the Balearic Sea and 20 from the Alboran Sea) and 10 from the Atlantic Ocean.

2.4. Statistical analyses

2.4.1. Relationship between coccolithophore assemblages and environmental variables

Prior to statistical analyses, environmental variables were checked for unimodal distribution. Only mixed layer depth, T_{ALK} and DIC were $\log_{10}$ transformed, since the transformation of other variables did not cause noticeable changes. Principal Component Analyses (PCA) was performed on this initial data set to assess the major environmental gradients and collinearity among the variables.

Coccolithophore relative abundances were square-root transformed to stabilize their variances. The species *Braarudosphaera* sp., *Calciosolenia* spp., *Coccolithus pelagicus* subsp. *braarudii*, *Coccolithus pelagicus* subsp. *pelagicus*, *and Pontosphaera* spp., were excluded from

138 the modern (and consequently from the fossil) coccolithophore assemblages since their
139 maximum relative abundance was not > 1 % in at least two samples. Detrended Correspondence
140 Analysis (DCA) was then performed on the modern coccolithophore assemblage to estimate the
141 length of the environmental gradient. A length of the first DCA axis > 2 Standard Deviation
142 (SD) units indicates the unimodal responses of the organisms (Birks, 1995; Ter Braak and
143 Prentice, 1988), while shorter lengths indicate linear responses.

144 Akaike's information criterion (AIC) was used in an ordination analysis to identify the
145 minimum number of variables (subset) that, being statistically significant, explained the
146 maximum variation in the modern coccolithophore assemblage. Canonical Correspondence
147 Analysis (CCA) was used to evaluate the influence of this environmental subset to explain
148 coccolithophore distribution in the modern training set.

149 The ratio between the first constrained axis and the first unconstrained axis (λ_1/λ_2) was used
150 as a diagnosis to test the strength of a single environmental variable when the effects of those
151 remaining were excluded from the analyses (ter Braak and Juggins, 1993). If $\lambda_1/\lambda_2 \geq 1$, the
152 variable under study is considered to be important for explaining the distribution of the species.
153 The proportion of the variance in the coccolithophore training set explained uniquely by each
154 significant environmental variable was calculated using variance partitioning.

155 Ordination analyses and variance partitioning were performed using the 'vegan' package
156 v.2.3. (Oksanen et al., 2015) for R (R Core Team, 2015).

157 *2.4.2. Transfer function*

158 Calibration models were calculated for the variable of interest (and each variable by means
159 of exploratory analysis) using the weighted-averaging-partial least squares (WA-PLS) method
160 (ter Braak and Juggins, 1993; ter Braak et al., 1993) and the Modern Analog Technique (MAT)
161 (Prell, 1985), both implemented in C2 version 1.4.3 software (Juggins, 2007). All models were
162 calculated for the cross-validation predictions by bootstrapping (999 permutation cycles) (Birks,
163 1995). In MAT, the number of analogs resulting in the maximum coefficient of determination
164 (R^2_{boot}) between the observed and predicted values and the lowest root-mean square error of
165 prediction (RMSEP) (Telford et al., 2004) was calculated using an optimization set together
166 with the usual training and test sets implemented in the 'analoge' package for R (R Core Team,
167 2015). In WA-PLS, a decrease of 5 % or more in RMSEP was required to retain the next
168 component (Birks, 1995; ter Braak et al., 1993).

169 Many coccolithophore species inhabit at depths within a specific range of the photic zone
170 and are subject to environmental seasonality (Winter et al., 1994). Therefore, the depth and
171 season considered for calibration and reconstruction should be those that most influenced the
172 coccolithophore fossil assemblage. Following the procedure described by Telford et al. (2013),

we reconstructed the variable of interest based on summer-, winter- and annual-averaged data at 9 different depths of the photic zone from 10 to 200 m using the 'paleoSig' package v.1.1-1 (Telford, 2012) for R (R Core Team, 2015). The reconstruction that explains the highest proportion of variance in the fossil data being statistically significant reflects the depth and season that most influenced the coccolithophore fossil assemblage and hence provides the most suitable calibration.

Outliers may reduce the power of prediction of the calibration model as well as introducing undesirable effects in model coefficients (Birks, 1995). Potential outliers were determined as those whose absolute residual was higher than the mean SD of the observed values (Edwards et al., 2004).

A combination of the highest R^2_{boot} and the lowest RMSEP was used as a criterion for the quality prediction of the model. The graphical representations of the observed values against the values predicted by the model and the residuals against the predicted values were used as a diagnosis of the model.

2.4.3. Derived reconstruction and evaluation

MAT and WA-PLS were applied to the fossil coccolithophore assemblages of core CEUTA10PC08, which were previously square-root transformed, using C2 version 1.4.3 software (Juggins, 2007). Sample-specific reconstruction errors under bootstrapping were derived automatically by C2 software, considering the prediction error due to: i) errors in estimating species coefficients, and ii) errors in the calibration function (further details may be found in Birks et al. (1990)). In order to assess the quality of the modern analogs for the fossil (downcore) samples, the squared chord distance between each fossil sample and each sample in the modern training set (Overpeck et al., 1985) was calculated with MAT by C2 software. A squared chord distance below the 10^{th} percentile would be considered good, while values above this cutoff would represent assemblages with poor analogs (Simpson, 2007).

The first axis of the PCA analyses of the fossil dataset ($PC1_{fossil}$) shows the most important changes in the composition of the fossil coccolithophore assemblage. Comparison between $PC1_{fossil}$ and the reconstructed variable of interest was used to assess whether the reconstruction could be considered representative of the major ecological changes of the fossil assemblage (Juggins, 2013).

3. RESULTS

3.1. Geographical distribution of coccolithophores

206 The small placoliths (small *Gephyrocapsa* and *E. huxleyi* < 4 μm) are the dominant taxa (Fig.
207 2b, c) constituting on average 83 % of coccolithophore assemblages. Small *Gephyrocapsa*
208 shows higher abundances near the Spanish coast and southeast of the Balearic Islands. *E.*
209 *huxleyi* < 4 μm is more abundant in the Balearic Sea and around the Ebro River Delta (Fig. 2c).
210 *G. muellerae* (Fig. 2d) concentrates southeast of the Balearic Islands and shows a patch of 2 %
211 in the northern Alboran Sea. *C. leptoporus* and *Helicosphaera* spp. (Fig. 2e, f) are almost absent
212 in the Alboran Sea and show similar patchy distributions between the Catalan and the Balearic
213 fronts and east of the Balearic Islands. *F. profunda* (Fig. 2g) is more abundant in the Atlantic
214 Ocean (up to 16 %) and gradually decreases eastward. It shows two patches (up to 4 %) south of
215 the Ebro River mouth. *G. oceanica* (< 5 μm) (Fig. 2h) is mostly distributed near the Strait of
216 Gibraltar. It also shows a patch (up to 3 %) around the Andarax River mouth.

217 **3.2. Relationship between coccolithophores and environmental variables**

218 The PC1 explains 56.1 % of the variance within the environmental data set (Fig. 3a) and is
219 highly correlated with CO_3^{2-}, salinity, pH and T_{ALK}. PC2 explains 22.3 % of the total variance
220 and primarily summarizes the information on temperature and phosphate.

221 The ordination based on the AIC revealed that only salinity, nitrate, phosphate, silicate and
222 oxygen are needed to explain the maximum variation in the modern coccolithophore
223 assemblage and are significant at the 95 % level when added individually to the model via a
224 forward selection procedure. The first axis of the DCA performed on the modern
225 coccolithophore assemblage was 2.6 SD units. Accordingly, unimodal methods were followed.
226 The CCA (Fig. 3b) revealed sites and species distribution along this environmental subset. The
227 others were also plotted as passive variables to avoid overfitting. The vectors show that salinity
228 exhibits the longest gradient and is strongly correlated with the CCA1, indicating a strong
229 relationship with coccolithophore distribution. Some sites from the Alboran and Balearic Seas
230 and the taxa medium *Gephyrocapsa* and *E. huxleyi* (> 4 μm) were found to be distributed along
231 the CCA2. Individual CCAs (Table 1) to calculate λ_1/λ_2 showed that salinity was the most
232 important variable among those found to be significant. Variance partitioning revealed that
233 these significant variables accounted for 38.9 % of the cumulative variance in the
234 coccolithophore training set and salinity explained a large proportion of this variance (15.5 %).

235 **3.3. Transfer functions**

236 Salinity explained the largest amount of variation in the coccolithophore assemblages and
237 was therefore chosen to develop the coccolithophore-based transfer function. Additionally,
238 comparison among the R^2_{boot} from preliminary calibration models for each variable confirmed
239 the best predictive power for salinity (Table 1).

240 Among the WA-PLS models for salinity, the two-component model (WA-PLS2) was chosen
241 as the most suitable since it afforded a reduction of 6.4 % in the RMSEP. The ideal number of
242 analogs for MAT was six.

243 The analyses of the amount of down-core variance explained by the summer, winter, and
244 annual salinity reconstructions at 9 different depths and their statistical significance revealed
245 that the mean-annual reconstruction at 10 m explained the highest variance. Hence, the
246 reconstruction for core CEUTA10PC08 was based on the mean-annual salinity data at 10 m
247 depth and referred to as SSS reconstruction.

248 Five samples showed higher residuals than the SD of salinity and were preliminary identified
249 as potential outliers (supplementary material). However, only one of these samples (CO-81-
250 2/TK-2) was identified as an outlier in both MAT and WA-PLS regression methods. This had a
251 bright yellowish color under the microscope, likely due to the effect of diagenetic processes. In
252 order to retain the maximum number of observations representing modern environmental
253 conditions, only this sample was removed from subsequent model implementations, leading to
254 an improvement of the MAT and WA-PLS2 R^2_{boot} coefficient of 3.4 % and 6.6 %, respectively,
255 and reducing both Max_Bias_{boot} and RMSEP (Table 2).

256 The final MAT and WA-PLS2 models showed similar quality predictions (Table 2). The
257 salinity values in the modern training set vary from 36.2 to 38.2 psu. Intermediate values (37.1-
258 37.6 psu) are less well represented by the observations (Fig 4a). MAT- and WA-PLS2-predicted
259 values are shown in Figs. 4b, c. The predicted *versus* observed values from both models
260 approach the diagonal of slope one (which indicates perfect predictions) reasonably well (Fig.
261 4d, e). The residuals for the MAT and WA-PLS2 models (Fig. 4f, g) are equally distributed
262 around zero and show no apparent trends.

263 **3.4. SSS reconstruction**

264 SSS trends and values reconstructed for the CEUTA10PC08 core derived from both MAT
265 and WA-PLS2 are very similar (Fig. 5a, b). These only differ during the stadials associated with
266 Heinrich Events 2 and 1 (H2 and H1), when the WA-PLS2-estimated SSS shows more
267 pronounced salinity decreases.

268 The SSS reconstructions obtained from core CEUTA10PC08 (Fig. 5a) can be divided into
269 three intervals: i) the period from 25.5 to 15.5 ka is characterized by higher values that oscillate
270 between 37.8 and 37 psu. Lower values are found from 20 to 18 ka, followed by a drop of 0.8
271 psu at 17.3 ka; ii) the period from 15.5 to 9 ka shows fast, large-amplitude changes. An abrupt
272 decrease from 37.9 to 36.9 psu can be recognized at 15 ka, followed by large peaks of high
273 values at 12.8, 11.1, and 10.2 ka; and iii) the period from 9 to 4.5 ka records the lowest values,
274 which vary between 37 and 36.5 psu, and shows a general decreasing trend.

On average, the errors associated with both SSS reconstruction are of a similar magnitude: ±0.15 psu for MAT and ±0.17 psu for WA-PLS (Fig. 5a). Squared chord distances between fossil and modern assemblages (Fig. 5b) revealed that many samples from 25.5 to 16 ka were above the 10th percentile. A comparison between $PC1_{fossil}$ and the SSS reconstruction is depicted in Fig. 5c, showing general good agreement, especially for the last 16 kyr.

4. DISCUSSION

4.1. Geographic coccolithophore distribution and SSS

E. huxleyi (< 4 μm) and small *Gephyrocapsa* are widespread in the Western Mediterranean, as previously reported for surface sediment and water column samples (Álvarez et al., 2010; Knappertsbusch, 1993; Oviedo et al., 2015). These taxa, especially *E. huxleyi* (< 4 μm), are cosmopolitan and tolerate wide ranges of temperature and salinity (Winter et al., 1994). *G. muellerae* abundance is higher southeast of the Balearic Islands, where the MAW encounters more saline and warmer Mediterranean waters, and close to the Alboran Front, possibly reflecting its preference for rich-nutrient waters, as reported for sediment trap samples in the Alboran Sea (Bárcena et al., 2004; Hernández-Almeida et al., 2011). *C. leptoporus* and *Helicosphaera* spp. (Fig. 2e, f) show similar spatial distributions and abundances. Interestingly, the CCA suggests that *Helicosphaera* spp. have a preference for more saline waters (Fig. 3b). By contrast, in paleoceanographic works this species has been linked to fresher and turbid waters in the Mediterranean Sea (Ausín et al., 2015; Colmenero-Hidalgo et al., 2004; Grelaud et al., 2012). *Helicosphaera* spp. abundance in surface sediments from the northeastern Balearic Island has also been related to upwelling events (Álvarez et al., 2010). Similarly, the abundance of *C. leptoporus* in the Alboran Sea has been linked to nutrient-rich waters (Bárcena et al., 2004). The similar patchy pattern shown by both species may be related to the temporary upwelling of nutrient-rich waters associated with frontal structures in the area limited by the Balearic and Catalan fronts (Font et al., 1988). In agreement with this interpretation, the co-occurrence of both species in other Mediterranean locations has already been linked to high coccolithophore productive periods and pre-upwelling events (Hernández-Almeida et al., 2011; Ziveri et al., 2000). The CCA (Fig. 3b) suggests that *F. profunda* and *G. oceanica* (< 5 μm) woul be associated to less saline waters. This notion may partly be a consequence of their higher abundance in Atlantic waters (Fig. 2d). *G. oceanica* has already been proposed as a tracer for AW influx in the Western Mediterranean Sea (Álvarez et al., 2010; Bárcena et al., 2004; Knappertsbusch, 1993; Oviedo et al., 2015). Similarly, the *F. profunda* spatial distribution reflects the path of the Algerian current (Fig. 2a, d), formed by recent and fresher MAW (Fig. 2a, d). Low percentages of *F. profunda* spottily distributed south of the Ebro River and in the Catalan-Balearic Sea suggest this species may be also affected by the influence of river

discharges (Álvarez et al., 2010). These results suggest that *F. profunda* and *G. oceanica* proliferate mainly in waters of Atlantic origin, but not exclusively, as indicated by their presence in the Eastern Mediterranean (Knappertsbusch, 1993; Malinverno et al., 2008) where Atlantic influence becomes diluted.

Salinity was highly correlated with CO_3^{2-} and pH (Fig. 3a, b). Oviedo et al. (2015) have found exactly the same variables as being the most important factors to account for changes in heterococcolithophore assemblages from the study of coccolithophore distribution from water column samples and *in situ* environmental measurement in the Mediterranean Sea. In our study, multivariate analyses revealed that salinity was significant and was the most important variable of those studied in explaining the variance in coccolithophore data in this modern training set. However, the individual importance and proportion of variance explained by each of the significant variables was not assessed in the study of Oviedo et al. (2015). Despite this, the authors discarded salinity as a final explanatory variable, arguing that *E. huxleyi*, the most abundant and ubiquitous extant coccolithophore (Cros and Fortuño, 2002), inhabits at a wide salinity range, suggesting a negligible ecological effect of salinity on coccolithophores. Contrary to this reasoning, the direct relationship between varying salinities and the morphology of *E. huxleyi* has been demonstrated by several authors (Bollmann and Herrle, 2007; Bollmann et al., 2009; Fielding et al., 2009; Green et al., 1998; Paasche et al., 1996; Schouten et al., 2006) in both culture experiments and marine surface sediment samples. Oviedo et al. (2015) later explained the high and negative relationship that they found between salinity and *G. oceanica*, *G. muellerae* and *E. huxleyi* morphotype B/C distributions as being a consequence of their carry-over by the AW through the Mediterranean. Instead of this, however, we interpret the AW influx as promoting the optimal conditions for these species to thrive in the Mediterranean Sea. Therefore, the coccolithophore relationship with salinity would reflect the different water masses where coccolithophore species prefer to inhabit.

It is worth mentioning that salinity influences the solubility of CO_3^{2-} via several pathways: the solubility of free carbon dioxide in water, the solubility product constants, the concentration of hydrogen ions, and the quantity of calcium in the water (Trask, 1936). Accordingly, salinity could influence coccolithophores through coccolith calcification processes. In contrast, Bollmann and Herrle, (2009) have proposed that salinity influences coccolithophores through cell turgor regulation linked to osmotic processes. Although there is no clear consensus about the mechanism through which salinity influences coccolithophores, many other studies point to a strong influence of this variable on molecular compounds only produced by coccolithophores and on specific species. In the Japan Sea, salinity has been proposed to have an ecological or physiological influence on the production of alkenone and alkenoates, which are organic compounds mainly produced by the genera *Emiliania* and *Gephyrocapsa* (Fujine et al., 2006).

In the Baltic Sea, alkenone unsaturation ratios have been found to be significantly correlated with salinity (Blanz et al., 2005). In the Mediterranean Sea, Knappertsbusch (1993) found that *G. oceanica* distribution was linearly correlated with salinity. Based on such evidences, we propose that the assemblage composition may be conditioned by the optimum salinity range preferred by each species. Moreover, salinity has proved to be important to other marine unicellular planktonic groups such as diatoms (Jiang et al., 2014; Li et al., 2012) and dinoflagellate cysts (Jansson et al., 2014, and references therein), reinforcing the hypothesis of salinity as an important variable for planktonic communities in semi-enclosed basins.

4.2. Transfer function quality

A general good fit can be deduced for both models, although MAT was seen to perform slightly better from a higher R^2_{boot} and a lower RMSEP (Table 2) and plotted predicted values compared with observed values (Fig. 4). Intermediate salinity values (37.1- 37.6 psu) are less well represented than the more extreme values (Fig. 4d, e). Unevenness can bias the RMSEP leading to overestimation of the predictive power of the model (Telford and Birks, 2011).While an even distribution would be always desirable, unevenness is a feature inherent to most training sets from oceanic environments. In this case, it is not severe and the observations, although unevenly distributed along the salinity gradient, do not leave gaps. The distribution of the residuals (Fig. 4f, g) indicates the adequacy of the model.

4.3. Downcore SSS reconstruction

The derived MAT and WA-PLS2 SSS reconstructions (Fig. 5a) are very similar. Nevertheless, WA-PLS2 shows more marked salinity decreases than MAT during the H2 (25.2-23.7 ka) and H1 (17.4-15.9 ka). Unlike WA-PLS, MAT does not consider the entire dataset when calculating the species optima, only the most taxonomically similar analogs, and is more sensitive to local conditions (Telford and Birks, 2009). Fossil samples lack good analogs for the H2 and H1, coinciding with large peaks of *E. huxleyi* (> 4 μm) (Fig. 5b). H2 and H1 have been linked to the entry of cold and fresher water originating from the North Atlantic ice melting in the Western Mediterranean Sea (Cacho et al., 1999; Melki, 2011; Sierro et al., 2005), suggesting the preference of *E. huxleyi* (> 4 μm) not only for cold waters (Colmenero-Hidalgo et al., 2002; Colmenero-Hidalgo et al., 2004) but also fresher waters in the past. By contrast, Bollmann and Herrle, (2007) reported a current positive correlation between the size of *E. huxleyi* up to 4 μm and increasing salinities from the study of globally distributed core-top samples. These authors used this relationship to estimate salinity values during the LGM. Interestingly, they observed several overestimations with regard to other published values in samples characterized by high relative abundances of larger specimens of *E. huxleyi* (> 4 μm). These discrepancies suggest that *E. huxleyi* (> 4 μm) in ancient sediments lacks an analog in modern assemblages, as indicated

by the high dissimilarity between fossil samples with high percentages of this species and modern samples (Fig. 5b).

Because MAT is strongly dependent upon on the analogs selected (Telford and Birks, 2009) and since the WA-PLS2 reconstruction for H2 and H1 is more coherent with a freshwater inflow scenario, it seems that WA-PLS2 affords more reliable values than MAT. Consequently, WA-PLS2-estimated SSS was chosen for our final interpretations.

Transfer functions assume that the ecological response of organisms to either the environmental variable of interest or to the linear combination of this important variable with others has not changed significantly over the time span represented by the fossil assemblage (Birks, 1995). The good agreement observed between $PC1_{fossil}$ and the reconstructed SSS patterns from 16 ka onwards (Fig. 5c) suggests that the SSS transfer function fulfills this assumption back to 16 ka. Larger differences are observed from 25 to 16 ka, possibly promoted by the lack of analogs during this time span, discussed above. Consequently, the SSS reconstruction from 25 to 16 ka will not be discussed further.

4.4. SSS changes in the Alboran Sea over the last 15.5 kyr

4.4.1. Termination 1b (T1b)

A decrease in salinity of about 0.6 ± 0.15 psu occurred from 15.4 to 14.6 ka (Fig. 6a). The global sea-level rise of ~20 m during meltwater pulse 1a (mwp-1a) has been dated between 14.6 and 14 ka (Stanford et al., 2006, and references therein). Since this section covers 3,000 yr with no control point (Fig. 6a), it could be an artifact of poorly constrained chronology for this time interval. Nevertheless, this seems unlikely because other authors (Duplessy et al., 1992; Emeis et al., 2000; Kallel et al., 1997) have reported SSS decreases in different regions of the Mediterranean Sea and Atlantic Ocean at this time from a combination of oxygen isotope ($\delta^{18}O$) and SST data. These salinity decreases are larger than that observed for the CEUTA10PC08 core. For instance, Duplessy et al. (1992) identified a salinity drop of about 2.5 psu in an Atlantic core west of the Strait of Gibraltar. It is worth mentioning that the salinity changes estimated by this method depend strongly on the accuracy of the SST record (Schmidt, 1998) and the unknown salinity-seawater $\delta^{18}O$ relationship in the past (Rohling, 1999), being sensitive to several deviations and uncertainties that are difficult to assess (Rohling, 2000; Rohling and Bigg, 1998; Schmidt, 1999). Although the uncertainty in the chronology prevents a robust correlation, the smaller SSS decrease identified in the SSS reconstruction could be related to the Laurentide ice sheet melting and retreat at ~15.5 ka (Clark et al., 2001). This event has already been proposed to be the cause of the freshwater input identified at 15.3 ka south of Iceland via advection within the North Atlantic Current

(NAC) and subsequently its northern branch (Thornalley et al., 2010). Similarly, the southeastern branch of NAC could have advected freshwater to the study area.

4.4.2. Bølling–Allerød (B–A)

The SSS values are generally low for the B–A, the Bølling being fresher than the Allerød (Fig. 6a). Owing to the global sea-level rise during the B–A, a greater volume of AW would have entered through the Strait, decreasing the average SSS. This period of reduced salinity also coincides with the highest values of total concentration of C_{37} alkenones, a proxy of organic matter preservation, from a nearby core located off the coast of Malaga (Ausín et al., 2015) (Fig. 6b). This accumulation of high amounts of organic matter resulted in the formation of the so-called Organic-Rich Layer (ORL-1) (Cacho et al., 2002) in the Western Mediterranean, although its origin is still under debate (Rogerson et al., 2008; Rohling et al., 2015). The joint effect of a salinity reduction of 0.8 psu and a temperature increase of 3 ºC (Cacho et al., 2001) (Fig. 6c) would have led to a significant reduction in sea surface density, possibly prompting stagnation of the upper water column. This, along with increased organic matter export to the seabed (Ausín et al., 2015) and reduced deep-basin ventilation (Martínez-Ruiz et al., 2015), would have hampered organic matter mineralization, reinforcing the formation of the ORL-1 in the Alboran Sea. According to Rohling et al. (2015), the origin of ORL-1 lies in hydraulic changes in the Strait of Gibraltar (Bernoulli aspiration depth) and/or the inhibition of deep water formation in the Gulf of Lion, both resulting from a drastic reduction in seawater density. Those authors have shown that the mwp-1a and the monsoon flooding into the Eastern Mediterranean were insufficient to trigger these mechanisms, and demonstrated that the Alpine melt-water input into the NW Mediterranean at this time (Ivy-Ochs et al., 2007) may have played an essential role as freshwater forcing.

4.4.3. Younger Dryas (YD) and the Holocene

The YD exhibits a shift from higher to lower SSS values, decreasing by a total of 0.6 psu along its two phases: YDa and YDb (Fig. 6a). Several large short-term SSS fluctuations occurred as from the onset of the YD throughout the early Holocene (up to 8 ka). This time span coincides with a sea level rise of ~ 30 m (Peltier and Fairbanks, 2006) due to short-lived freshwater inputs associated with residual melting of the northern hemisphere ice sheets (Andrews and Dunhill, 2004; Elmore et al., 2015; Seidenkrantz et al., 2013; Tornqvist and Hijma, 2012). Six brief periods of a SSS decreasing trend were identified at 12.77-12.06, 11.95-11.71, 11.24-11.00, 10.09-9.83, 9.30-9.12, and 8.95-7.90 ka (Fig. 6a). REDFIT spectral analysis reveals a periodicity of 770±40 years (Fig. 6d), very similar to the 730±40 years cycle found by Cacho et al. (2001) in a SST record in the Alboran Sea, which was punctuated by the so-called Alboran cooling (AC) events (Fig. 6c). Although this similarity does not necessarily imply a

450 causal relationship, the timing of SSS decreases is comparable to that of the AC events (Table
451 3), suggesting a common origin. Cacho et al. (2001) have associated the AC events to influxes
452 of cold Atlantic waters in the Alboran Sea during ice-rafted debris discharges (so-called Bond
453 events) (Bond et al., 1997) (Table 3). These latter authors noted that the oxygen isotopic record
454 showed no evidence of any of the coolings found for each Bond event during the Holocene and
455 argued that the cooler surface waters may have also been fresher, offseting the expected
456 temperature-driven $\delta^{18}O$ enrichment in their records. Similarly, the highly-resolved $\delta^{18}O$ profile
457 reported by Cacho et al. (2001) does not show any of the expected oxygen isotopic enrichments
458 associated with the AC events, supporting the presence of fresher waters at those times. We
459 suggest that freshwater advection (FA) events (as well as AC events) would have resulted from
460 the influx of fresher and colder Atlantic waters in the Alboran Sea related to the southeastward
461 drifting of meltwater from the Labrador, Greenland and Iceland seas (Bond et al., 1997).

462 FA events only occurred during the early Holocene, while AC and Bond events have also
463 been identified through the middle and late Holocene. Wenner et al. (2014) concluded that,
464 unlike those occurring later, early Holocene Bond events originated from changes in the
465 meridional overturning circulation due to meltwater pulses from the Northern Hemisphere ice-
466 sheets. It is likely that FA events would only have been noticeable when this mechanism was
467 operating (i.e. the early Holocene), since very little meltwater was present after that period
468 (Elmore et al., 2015).

469 An SSS increase of 0.87±0.15 psu is observed from 10.7 to 10 ka. Because the Western
470 Mediterranean is a semi-enclosed basin, local conditions may have played a role as additional
471 feedbacks for this rapid high-amplitude variability. For this brief period, Frigola et al. (2008)
472 have demonstrated the most pronounced weakening of the Mediterranean thermohaline
473 circulation for the last 50 ka. The consequent reduction in Atlantic-Mediterranean water
474 exchange, along with the maximum summer insolation and inland aridity (Fletcher et al., 2010),
475 would have led to more saline surface waters.

476 FA1 includes the 8.2 ka event (Alley et al., 1997), which has been linked to a sub-
477 thermocline freshening of 0.5 psu in the North Atlantic (Thornalley et al., 2009). However, no
478 distinctive SSS changes are observed in relation to this event, suggesting that it would have had
479 a negligible effect on surface salinity in the Alboran Sea. Minimum SSS values are recorded at
480 7.8 ka, possibly related to maximum high-stand conditions reached at 7.4 ka (Zazo et al., 2008),
481 along with the influence of the African Humid Period (AHP; 11-5.5 ka) over the study area,
482 especially up to its decline at 7.4 ka (deMenocal et al., 2000). From 7.8 to 4.5 ka, salinity values
483 level off around 36.6 psu, close to present SSS values.

484 **5. CONCLUSIONS**

Multivariate statistical analyses show that coccolithophore distribution of modern coccolithophore assemblages in the Atlantic Ocean, west of the Strait of Gibraltar, and the Western Mediterranean was mainly influenced by annual mean salinity at 10 m depth. MAT and WA-PLS2 calibration models show similar outcomes. These models were applied to coccolithophore assemblages from a fossil core to reconstruct SSS at high resolution for the last 25 kyr in the Alboran Sea. Statistical analyses reveal assemblages lacking good modern analogs in relation to the species *E. huxleyi* > 4 μm during H2 and H1 and part of the LGM, preventing further interpretations for these periods. A low SSS was found for the B−A, possibly due to the post-glacial sea-level rise. The consequent reduction in sea surface density is suggested to have reinforced the formation of the ORL-1. During the YD and Holocene, six brief, abrupt SSS decreases at 12.77-12.06, 11.95-11.71, 11.24-11.00, 10.09-9.83, 9.30-9.12, and 8.95-7.90 ka were linked to the advection of fresher and colder AW related to the southeastward drifting of meltwater in the North Atlantic. No evidence of the 8.2 ka event is found in the reconstructed SSS, which reached its lowest values at 7.8 ka, coinciding with high-stand conditions in the Alboran Sea and the onset of the decline of the African Humid Period. SSS remained low from 7.8 to 4.5 ka, close to its present values.

A broader understanding of the ecological link between coccolithophore species and environmental parameters would be desirable in order to be able to place coccolithophore-based transfer functions within the ecological context in future works. Nevertheless, the diverse statistical tests performed in this study and the strong emphasis placed on assessing the validity and reliability of both the model and the reconstruction do reveal the potential of coccolithophores for developing transfer functions. The derived transfer function provides a potential independent proxy for quantitative reconstructions of SSS changes in other locations of the Western Mediterranean Sea over the last 15.5 kyr.

Acknowledgements

We thank two anonymous reviewers for their critical discussion to improve this manuscript. B. Ausín is sincerely grateful to the Core Repository of the Institute of Marine Sciences- CSIC at Barcelona and the University of Vigo for the core-top samples supply. This study was supported by the FPU grant AP2010-2559 of the Spanish Ministry of Education given to B. Ausín and by the Consolider Ingenio "GRACCIE" program CSD 2007-00067, the program SA263U14 of Junta de Castilla y León, and the programs: CGL2011-26493, VACLIODP339, CTM2008-06399-C04/MAR, CTM 2012-39599-C03-02/03 and MOWER (CTM 2012-39599-CO3-02/03) of the Spanish Ministry of Economy and Competitiveness.

References

519 Álvarez MC, Amore FO, Cros L, Alonso B and Alcántara-Carrió J: Coccolithophore
520 biogeography in the Mediterranean Iberian margin, Revista Española de
521 Micropaleontología, 42, 359-372, 2010.
522 Alley RB, Mayewski PA, Sowers T, Stuiver M, Taylor KC and Clark PU: Holocene climatic
523 instability: A prominent, widespread event 8200 yr ago, Geology, 25, 483-486,
524 1997.
525 Andrews JT and Dunhill G: Early to mid-Holocene Atlantic water influx and deglacial
526 meltwater events, Beaufort Sea slope, Arctic Ocean, Quaternary Research, 61, 14-
527 21, 2004.
528 Ausín B, Flores JA, Bácena MA, Sierro FJ, Francés G, Gutiérrez-Arnillas E, Hernández-
529 Almeida I, Martrat B, Grimalt JO and Cacho I: Coccolithophore productivity and
530 surface water dynamics in the Alboran Sea during the last 25 kyr, Palaeogeography,
531 Palaeoclimatology, Palaeoecology, 418, 126-140, 2015.
532 Bárcena MA, Flores JA, Sierro FJ, Pérez-Folgado M, Fabres J, Calafat A and Canals M:
533 Planktonic response to main oceanographic changes in the Alboran Sea (Western
534 Mediterranean) as documented in sediment traps and surface sediments, Marine
535 Micropaleontology, 53, 423-445, 2004.
536 Baumann KH, Andruleit H, Boeckel B, Geisen M and Kinkel H: The significance of extant
537 coccolithophores as indicators of ocean water masses, surface water temperature,
538 and palaeoproductivity: a review, Palaeontologische Zeitschrift, 79, 93-112, 2005.
539 Beaufort L, de Garidel-Thoron T, Mix AC and Pisias NG: ENSO-like Forcing on Oceanic
540 Primary Production During the Late Pleistocene, Science, 293, 2440-2444, 2001.
541 Beaufort L, Lancelot Y, Camberlin P, Cayre O, Vincent E, Bassinot F and Labeyrie L:
542 Insolation Cycles as a Major Control of Equatorial Indian Ocean Primary
543 Production, Science, 278, 1451-1454, 1997.
544 Bèthoux JP: Budgets of the Mediterranean Sea. Their dependance on the local climate and
545 on the characteristics of the Atlantic waters· Oceanologica Acta, 2, 157-163, 1979.
546 Birks HJB: Quantitative palaeoenvironmental reconstructions, in: Statistical Modelling of
547 Quaternary Science Data, technical guide 5, edited by: Maddy D and Brew JS.
548 Quaternary Research Association, Cambridge, 271 pp., 1995.
549 Birks HJB, Line JM, Juggins S, Stevenson AC and Braak CJFT: Diatoms and pH
550 Reconstruction, Philosophical Transactions of the Royal Society of London. Series
551 B, Biological Sciences, 327, 263-278, 1990.
552 Blanz T, Emeis K-C and Siegel H: Controls on alkenone unsaturation ratios along the
553 salinity gradient between the open ocean and the Baltic Sea, Geochimica et
554 Cosmochimica Acta, 69, 3589-3600, 2005.
555 Bollmann J and Herrle JO: Morphological variation of *Emiliania huxleyi* and sea surface
556 salinity, Earth and Planetary Science Letters, 255, 273-288, 2007.
557 Bollmann J, Herrle JO, Cortés MY and Fielding SR: The effect of sea water salinity on the
558 morphology of *Emiliania huxleyi* in plankton and sediment samples, Earth and
559 Planetary Science Letters, 284, 320-328, 2009.
560 Bond G, Showers W, Cheseby M, Lotti R, Almasi P, deMenocal P, Priore P, Cullen H,
561 Hajdas I and Bonani G: A Pervasive Millennial-Scale Cycle in North Atlantic
562 Holocene and Glacial Climates, Science, 278, 1257-1266, 1997.
563 Boyer TP, Antonov JI, Baranova OK, Coleman C, Garcia HE, Grodsky A, Johnson DR,
564 Locarnini RA, Mishonov AV, O'Brien TD, Paver CR, Reagan JR, Seidov D,
565 Smolyar IV and Zweng MM: World Ocean Database 2013, NOAA Atlas NESDIS
566 72, in: Silver Spring, MD, edited by: Levitus S and Mishonov A. 209 pp., 2013.
567 Cacho I, Grimalt JO and Canals M: Response of the Western Mediterranean Sea to rapid
568 climatic variability during the last 50,000 years: a molecular biomarker approach,
569 Journal of Marine Systems, 33-34, 253-272, 2002.
570 Cacho I, Grimalt JO, Canals M, Sbaffi L, Shackleton NJ, Schönfeld J and Zahn R:
571 Variability of the western Mediterranean Sea surface temperature during the last

572 25,000 years and its connection with the Northern Hemisphere climatic changes,
573 Paleoceanography, 16, 40-52, 2001.
574 Cacho I, Grimalt JO, Pelejero C, Canals M, Sierro FJ, Flores JA and Shackleton N:
575 Dansgaard-Oeschger and Heinrich Event Imprints in Alboran Sea
576 Paleotemperatures, Paleoceanography, 14, 698-705, 1999.
577 Clark PU, Marshall SJ, Clarke GKC, Hostetler SW, Licciardi JM and Teller JT: Freshwater
578 forcing of abrupt climate change during the last glaciation, Science, 293, 283-287,
579 2001.
580 Colmenero-Hidalgo E, Flores J-A and Sierro FJ: Biometry of Emiliania huxleyi and its
581 biostratigraphic significance in the Eastern North Atlantic Ocean and Western
582 Mediterranean Sea in the last 20,000 years, Marine Micropaleontology, 46, 247-263,
583 2002.
584 Colmenero-Hidalgo E, Flores JA, Sierro FJ, Bárcena MÁ, Löwemark L, Schönfeld J and
585 Grimalt JO: Ocean surface water response to short-term climate changes revealed by
586 coccolithophores from the Gulf of Cadiz (NE Atlantic) and Alboran Sea (W
587 Mediterranean), Palaeogeography, Palaeoclimatology, Palaeoecology, 205, 317-336,
588 2004.
589 Cros L and Fortuño J-M: Atlas of northwestern Mediterranean coccolithophores, Scientia
590 Marina, 66, 7–182, 2002.
591 deMenocal P, Ortiz J, Guilderson T, Adkins J, Sarnthein M, Baker L and Yarusinsky M:
592 Abrupt onset and termination of the African Humid Period: rapid climate responses
593 to gradual insolation forcing, Quaternary Science Reviews, 19, 347-361, 2000.
594 Duplessy JC, Labeyrie L, Arnold M, Paterne M, Duprat J and van Weering TCE: Changes in
595 surface salinity of the North Atlantic Ocean during the last deglaciation, Nature, 358,
596 485-488, 1992.
597 Edwards RJ, van de Plassche O, Gehrels WR and Wright AJ: Assessing sea-level data from
598 Connecticut, USA, using a foraminiferal transfer function for tide level, Marine
599 Micropaleontology, 51, 239-255, 2004.
600 Elmore AC, Wright JD and Southon J: Continued meltwater influence on North Atlantic
601 Deep Water instabilities during the early Holocene, Marine Geology, 360, 17-24,
602 2015.
603 Emeis K-C, Struck U, Schulz H-M, Rosenberg R, Bernasconi S, Erlenkeuser H, Sakamoto T
604 and Martinez-Ruiz F: Temperature and salinity variations of Mediterranean Sea
605 surface waters over the last 16,000 years from records of planktonic stable oxygen
606 isotopes and alkenone unsaturation ratios, Palaeogeography, Palaeoclimatology,
607 Palaeoecology, 158, 259-280, 2000.
608 Fatela F and Taborda R: Confidence limits of species proportions in microfossil
609 assemblages, Marine Micropaleontology, 45, 169-174, 2002.
610 Fielding SR, Herrle JO, Bollmann J, Worden RH and Montagnesd DJS: Assessing the
611 applicability of *Emiliania huxleyi* coccolith morphology as a sea-surface salinity
612 proxy, Limnology and Oceanography, 54, 1475–1480, 2009.
613 Fletcher WJ, Sánchez Goñi MF, Peyron O and Dormoy I: Abrupt climate changes of the last
614 deglaciation detected in a Western Mediterranean forest record, Climate of the Past,
615 6, 245-264, 2010.
616 Flores JA and Sierro FJ: Revised technique for calculation of calcareous nannofossil
617 accumulation rates, Micropaleontology, 43, 321-324, 1997.
618 Flores JA, Sierro FJ, Francés G, Vázquez A and Zamarreño I: The last 100,000 years in the
619 western Mediterranean: sea surface water and frontal dynamics as revealed by
620 coccolithophores, Marine Micropaleontology, 29, 351-366, 1997.
621 Font J, Salat J and Tintoré J.: Permanent features of the circulation in the Catalan Sea
622 (Northwestern Mediterranean), Oceanologica Acta, 9, 51-57, 1988.
623 Frigola J, Moreno A, Cacho I, Canals M, Sierro FJ, Flores JA and Grimalt JO: Evidence of
624 abrupt changes in Western Mediterranean Deep Water circulation during the last 50

kyr: A high-resolution marine record from the Balearic Sea, Quaternary International, 181, 88–104, 2008.
Fujine K, Yamamoto M, Tada R and Kido Y: A salinity-related occurrence of a novel alkenone and alkenoate in Late Pleistocene sediments from the Japan Sea, Organic Geochemistry, 37, 1074-1084, 2006.
García HE, Locarnini RA, Boyer TP, Antonov JI, Baranova OK, Zweng MM, Reagan JR and Johnson DR: World Ocean Atlas 2013, Volume 3: Dissolved Oxygen, Apparent Oxygen Utilization, and Oxygen Saturation, in: NOAA Atlas NESDIS 75, edited by: Levitus S and Mishonov A. 27 pp., 2014a.
García HE, Locarnini RA, Boyer TP, Antonov JI, Baranova OK, Zweng MM, Reagan JR and Johnson DR: World Ocean Atlas 2013, Volume 4: Dissolved Inorganic Nutrients (phosphate, nitrate, silicate), in: NOAA Atlas NESDIS 76, edited by: Levitus S and Mishonov A. 25 pp., 2014b.
Giraudeau J and Rogers J: Phytoplankton biomass and sea-surface temperature estimates from sea-bed distribution of nannofossils and planktonic foraminifera in the Benguela upwelling system, Micropaleontology, 40, 275–285, 1994.
Goyet C, Healy RJ and Ryan PD: Global distribution of total inorganic carbon and total alkalinity below the deepest winter mixed layer depths. ORNL/CDIAC-127, NDP-076. Carbon Dioxide Information Analysis Center, Oak Ridge National Laboratory, U.S. Department of Energy, Oak Ridge, Tennessee, 2000.
Green JC, Heimdal BR, Paasche E and Moate R: Changes in calcification and the dimensions of coccoliths of *Emiliania huxleyi* (Haptophyta) grown at reduced salinities, Phycologia: September, 37, 121-131, 1998.
Grelaud M, Marino G, Ziveri P and Rohling EJCPA: Abrupt shoaling of the nutricline in response to massive freshwater flooding at the onset of the last interglacial sapropel event, Paleoceanography, 27, PA3208, doi:3210.1029/2012PA002288, 2012.
Guerreiro C, Oliveira A, de Stigter H, Cachão M, Sá C, Borges C, Cros L, Santos A, Fortuño J-M and Rodrigues A: Late winter coccolithophore bloom off central Portugal in response to river discharge and upwelling, Continental Shelf Research, 59, 65-83, 2013.
Guerreiro C, Sá C, de Stigter H, Oliveira A, Cachão M, Cros L, Borges C, Quaresma L, Santos AI, Fortuño J-M and Rodrigues A: Influence of the Nazaré Canyon, central Portuguese margin, on late winter coccolithophore assemblages, Deep Sea Research Part II: Topical Studies in Oceanography, 104, 335-358, 2014.
Hernández-Almeida I, Bárcena MA, Flores JA, Sierro FJ, Sanchez-Vidal A and Calafat A: Microplankton response to environmental conditions in the Alboran Sea (Western Mediterranean): One year sediment trap record, Marine Micropaleontology, 78, 14-24, 2011.
Incarbona A, Di Stefano E, Patti B, Pelosi N, Bonomo S, Mazzola S, Sprovieri R, Tranchida G, Zgozi S and Bonanno A: Holocene millennial-scale productivity variations in the Sicily Channel (Mediterranean Sea), Paleoceanography, 23, PA3204, 2008.
Ivy-Ochs S, Kerschner H and Schlüchter C: Cosmogenic nuclides and the dating of Lateglacial and Early Holocene glacier variations: The Alpine perspective, Quaternary International, 164-165, 53-63, 2007.
Jansson I-M, Mertens KN, Head MJ, de Vernal A, Londeix L, Marret F, Matthiessen J and Sangiorgi F: Statistically assessing the correlation between salinity and morphology in cysts produced by the dinoflagellate *Protoceratium reticulatum* from surface sediments of the North Atlantic Ocean, Mediterranean-Marmara-Black Sea region, and Baltic-Kattegat-Skagerrak estuarine system, Palaeogeography, Palaeoclimatology, Palaeoecology, 399, 202-213, 2014.
Jiang H, Knudsen MF, Seidenkrantz M-S, Zhao M, Sha L and Ran L: Diatom-based reconstruction of summer sea-surface salinity in the South China Sea over the last 15,000 years, Boreas, 43, 208-219, 2014.

678 Juggins S: C2 Version 1.5 Software for ecological and palaeoecological data analysis and
679 visualisation, Newcastle University, Newcastle upon Tyne, UK, available at:
680 http://www.staff.ncl.ac.uk/stephen.juggins/software/C2Home.htm (last access: 7
681 July 2015), 2007.
682 Juggins S: Quantitative reconstructions in palaeolimnology: new paradigm or sick science?,
683 Quaternary Science Reviews, 64, 20-32, 2013.
684 Kallel N, Paterne M, Labeyrie L, Duplessy J-C and Arnold M: Temperature and salinity
685 records of the Tyrrhenian Sea during the last 18,000 years, Palaeogeography,
686 Palaeoclimatology, Palaeoecology, 135, 97-108, 1997.
687 Knappertsbusch M: Geographic distribution of living and Holocene coccolithophores in the
688 Mediterranean Sea, Marine Micropaleontology, 21, 219-247, 1993.
689 Li D, Knudsen MF, Jiang H, Olsen J, Zhao M, Li T, Knudsen KL, Seidenkrantz M-S and
690 Sha L: A diatom-based reconstruction of summer sea-surface salinity in the Southern
691 Okinawa Trough, East China Sea, over the last millennium, Journal of Quaternary
692 Science, 27, 771-779, 2012.
693 Locarnini R, Mishonov A, Antonov J, Boyer T, Garcia H, Baranova O, Zweng M, Paver CR,
694 Reagan JR, Johnson DR, Hamilton M and Seidov D: World Ocean Atlas 2013,
695 Volume 1: Temperature, in: NOAA Atlas NESDIS 73, edited by: Levitus S and
696 Mishonov A. 40 pp., 2013.
697 Malinverno E, Dimiza M, Triantaphyllou M, Dermitzakis M and Corselli C. (2008)
698 Coccolithophores of the Eastern Mediterranean sea: A look into the marine
699 microworld. Athens-GR: ION, 188.
700 Martínez-Ruiz F, Kastner M, Gallego-Torres D, Rodrigo-Gámiz M, Nieto-Moreno V and
701 Ortega-Huertas M: Paleoclimate and paleoceanography over the past 20,000 yr in
702 the Mediterranean Sea Basins as indicated by sediment elemental proxies,
703 Quaternary Science Reviews, 107, 25-46, 2015.
704 MEDOCGROUP: Observation of formation of deep water in the Mediterranean Sea, 1969,
705 Nature, 227, 1037-1040, 1970.
706 Melki T: Variation of deepwater convection in the western Mediterranean Sea (Gulf of Lion)
707 during the last 28 ka, Quaternary International, 241, 160-168, 2011.
708 Millot C: Circulation in the Western Mediterranean Sea, Journal of Marine Systems, 20,
709 423-442, 1999.
710 Monterey G and Levitus S: Seasonal Variability of Mixed Layer Depth for the World Ocean.
711 NOAA Atlas NESDIS 14, U.S. Gov. Printing Office, Wash., D.C., 96 pp, 1997.
712 Oksanen J, Blanchet FG, Kindt R, Legendre P, Minchin PR, O'Hara B, Simpson GL,
713 Solymos P, Stevens MHH and Wagner H: Vegan: Community Ecology Package, R
714 package version 2.3-0, 2015.
715 Overpeck JT, Webb T and Prentice IC: Quantitative interpretation of fossil pollen spectra:
716 Dissimilarity coeffi cients and the method of modern analogs, Quaternary Research,
717 23, 87–108, 1985.
718 Oviedo A, Ziveri P, Álvarez M and Tanhua T: Is coccolithophore distribution in the
719 Mediterranean Sea related to seawater carbonate chemistry?, Ocean Science, 11, 13-
720 32, 2015.
721 Paasche E, Brubak S, Skattebøl S, Young JR and Green JC: Growth and calcification in the
722 coccolithophorid *Emiliania huxleyi* (Haptophyceae) at low salinities, Phycologia:
723 September, 35, 394-403, 1996.
724 Peltier WR and Fairbanks RG: Global glacial ice volume and Last Glacial Maximum
725 duration from an extended Barbados sea level record, Quaternary Science Reviews,
726 25, 3322-3337, 2006.
727 Prell WL: The stability of low-latitude sea-surface temperatures: An evaluation of the
728 CLIMAP reconstruction with emphasis on the positive SST anomalies, Department
729 of Energy, Washington, D. C, 1985.

R Core Team: R: A language and environment for statistical computing, Viena, Austria, available at: http://www.R-project.org (last access: 28 July 2015), R Foundation for Statistical Computing, 2015.
Rogerson M, Cacho I, Jimenez-Espejo F, Reguera MI, Sierro FJ, Martinez-Ruiz F, Frigola J and Canals M: A dynamic explanation for the origin of the western Mediterranean organic-rich layers, Geochemistry, Geophysics, Geosystems, 9, Q07U01, doi: 10.1029/2007GC001936, 2008.
Rohling EJ: Environmental control on Mediterranean salinity and $\delta^{18}O$, Paleoceanography, 14, 706-715, 1999.
Rohling EJ: Paleosalinity: confidence limits and future applications, Marine Geology, 163, 1-11, 2000.
Rohling EJ and Bigg GR: Paleosalinity and $\delta^{18}O$: A critical assessment, Journal of Geophysical Research: Oceans, 103, 1307-1318, 1998.
Rohling EJ, Marino G and Grant KM: Mediterranean climate and oceanography, and the periodic development of anoxic events (sapropels), Earth-Science Reviews, 143, 62-97, 2015.
Saavedra-Pellitero M, Baumann KH, Hernández-Almeida I, Flores JA and Sierro FJ: Modern sea surface productivity and temperature estimations off Chile as detected by coccolith accumulation rates, Palaeogeography, Palaeoclimatology, Palaeoecology, 392, 534-545, 2013.
Saavedra-Pellitero M, Flores JA, Lamy F, Sierro FJ and Cortina A: Coccolithophore estimates of paleotemperature and paleoproductivity changes in the southeast Pacific over the past 27 kyr, Paleoceanography, 26, PA1201, doi: 1210.1029/2009PA001824, 2011.
Schlitzer R: Ocean Data View, http://odv.awi.de (last access: 22 July 2015), 2014.
Schmidt GA: Oxygen-18 variations in a global ocean model, Geophysical Research Letters, 25, 1201-1204, 1998.
Schmidt GA: Error analysis of paleosalinity calculations, Paleoceanography, 14, 422-429, 1999.
Schouten S, Ossebaar J, Schreiber K, Kienhuis MVM, Langer G, Benthien A and Bijma J: The effect of temperature, salinity and growth rate on the stable hydrogen isotopic composition of long chain alkenones produced by *Emiliania huxleyi* and Gephyrocapsa oceanica, Biogeosciences, 3, 113-119, 2006.
Seidenkrantz M-S, Ebbesen H, Aagaard--Sørensen S, Moros M, Lloyd JM, Olsen J, Knudsen MF and Kuijpers A: Early Holocene large-scale meltwater discharge from Greenland documented by foraminifera and sediment parameters, Palaeogeography, Palaeoclimatology, Palaeoecology, 391, Part A, 71-81, 2013.
Sierro FJ, Hodell DA, Curtis JH, Flores JA, Reguera I, Colmenero-Hidalgo E, Bárcena MA, Grimalt JO, Cacho I, Frigola J and Canals M: Impact of iceberg melting on Mediterranean thermohaline circulation during Heinrich events, Paleoceanography, 20, PA2019, doi: 2010.1029/2004PA001051, 2005.
Simpson GL: Analogue methods in palaeoecology: Using the analogue package, Journal of Statistical Software, 22, 2007.
Stanford JD, Rohling EJ, Hunter SE, Roberts AP, Rasmussen SO, Bard E, McManus J and Fairbanks RGCPA: Timing of meltwater pulse 1a and climate responses to meltwater injections, Paleoceanography, 21, PA4103, doi:4110.1029/2006PA001340, 2006.
Telford R: palaeoSig: significance tests of quantitative palaeoenvironmental reconstructions. R Package Version, 1.1-1., 2012.
Telford RJ, Andersson C, Birks HJB and Juggins S: Biases in the estimation of transfer function prediction errors, Paleoceanography, 19, PA4014, 2004.
Telford RJ and Birks HJB: Evaluation of transfer functions in spatially structured environments, Quaternary Science Reviews, 28, 1309-1316, 2009.

Telford RJ and Birks HJB: A novel method for assessing the statistical significance of quantitative reconstructions inferred from biotic assemblages, Quaternary Science Reviews, 30, 1272-1278, 2011.
Telford RJ, Li C and Kucera M: Mismatch between the depth habitat of planktonic foraminifera and the calibration depth of SST transfer functions may bias reconstructions, Clim. Past, 9, 859-870, 2013.
ter Braak CJF and Juggins S: Weighted averaging partial least squares regression (WA-PLS): an improved method for reconstructing environmental variables from species assemblages, Hydrobiologia, 269-270, 485-502, 1993.
ter Braak CJF, Juggins S, Birks HJB and van der Voet. H: Weighted averaging partial least squares regresion (WA-PLS): definition and comparison with other methods for species-environment calibration, chapter 25, in: Multivariate Environmental Statistics, edited by: Patil GP and Rao CR. Elsevier Science Publishers B.V., North-Holland, Amsterdam, 525-560 pp., 1993.
Ter Braak CJF and Prentice IC: A Theory of Gradient Analysis, in: Advances in Ecological Research, edited. Academic Press, 271-317 pp., 1988.
Thornalley DJR, Elderfield H and McCave IN: Holocene oscillations in temperature and salinity of the surface subpolar North Atlantic, Nature, 457, 711-714, 2009.
Thornalley DJR, McCave IN and Elderfield HCPA: Freshwater input and abrupt deglacial climate change in the North Atlantic, Paleoceanography, 25, PA1201, doi:1210.1029/2009PA001772, 2010.
Tornqvist TE and Hijma MP: Links between early Holocene ice-sheet decay, sea-level rise and abrupt climate change, Nature Geosci, 5, 601-606, 2012.
Trask PD: Relation of salinity to the calcium carbonate content of marine sediments, U.S. Geological Survey Professional Paper, 186-N, 273-299, 1936.
Wanner H, Mercolli L, Grosjean M and Ritz SP: Holocene climate variability and change; a data-based review, Journal of the Geological Society, doi:10.1144/jgs2013-1101, 2014.
Winter A, Jordan RW and Roth PH: Biogegraphy of living coccolithophores in ocean waters, in: Coccolithophores, edited by: Winter A and Siesser WG. University Press, Cambridge, 161-178 pp., 1994.
Zazo C, Dabrio CJ, Goy Goy JL, Lario J, Cabero del Río A, Silva Barroso PG, Bardají Azcárate T, Mercier N, Borja F and Roquero E: The coastal archives of the last 15 ka in the Atlantic–Mediterranean Spanish linkage area: Sea level and climate changes, Quaternary International, 181, 72-87, 2008.
Ziveri P, Rutten A, de Lange GJ, Thomson J and Corselli C: Present-day coccolith fluxes recorded in central eastern Mediterranean sediment traps and surface sediments, Palaeogeography, Palaeoclimatology, Palaeoecology, 158, 175-195, 2000.
Zweng MM, Reagan JR, Antonov JI, Locarnini RA, Mishonov AV, Boyer TP, Garcia HE, Baranova OK, Johnson DR, Seidov D and Biddle MM: World Ocean Atlas 2013, Volume 2: Salinity, in: NOAA Atlas NESDIS 74, edited by: Levitus S and Mishonov A. 39 pp., 2013.

Table 1.

Multivariate analyses results. λ_1/λ_2: individual CCA. Preliminary model coefficients from MAT and WA-PLS2. R^2_{boot}: bootstrapped coefficient of determination between the observed and predicted values. RMSEP: root mean square error of prediction.

			MAT		WA-PLS	
Variable	**λ_1/λ_2**	**% Explained variance**	**Boot_R^2**	**RMSEP**	**Boot_R^2**	**RMSEP**
*Salinity	1.38	15.47	0.83	0.30	0.75	0.33
*Nitrate	0.65	8.14	0.45	0.32	0.39	0.33
*Phosphate	0.25	4.89	0.36	0.02	0.19	0.02
*Silicate	0.22	8.93	0.56	0.24	0.40	0.26
*Oxygen	0.1	1.46	0.15	0.05	0.05	0.05
Chlorophyll-*a*			0.61	0.05	0.58	0.05
Temperature			0.12	0.52	0.07	0.53
Oxygen Saturation			0.20	1.04	0.18	1.02
Mixed Layer Depth			0.31	0.19	0.25	0.19
CO_3^{2-}			0.74	0.02	0.70	0.02
pH			0.70	0.02	0.67	0.02
T_{ALK}			0.70	0.00	0.67	0.004
DIC			0.51	13.31	0.48	13.16

*Variables determined by ordination based on AIC.

Table 2.

Model coefficients from final MAT and WA-PLS2 cross-validated by boot-strapping for SSS, after removal of one outlier. R^2_{boot}: bootstrapped coefficient of determination between the observed and predicted values. Max_Bias_{boot}: bootstrapped maximum bias. RMSEP: root mean square error of prediction (psu).

	MAT	**WA-PLS2**
$\mathbf{R^2_{boot}}$	0.85	0.80
$\mathbf{Max\_Bias_{boot}}$	0.23	0.22
RMSEP	0.29	0.30

Table 3.

Timing (given in ka cal. BP) of: freshwater advection events (FA) deduced from SSS decreases in the CEUTA10PC08 core (this study) and their magnitude; Alboran cooling (AC) events from core MD 95-2043 (ACYD-AC3, Cacho et al., (2001)); and Bond events in the North Atlantic (Bond et al., 1997).

SSS decreases	SSS change (psu)	AC events	Bond events
FAYD	0.79±0.15	ACYD	
12.77-12.06		13.1-12.0	12.5
FA5	0.22± 0.16	AC6	---
11.95-11.71		11.9-11.65	
FA4	0.41± 0.16	AC5	
11.24-11.00		11.21-10.95	11.1
FA3	1.0± 0.15	AC4	
10.09-9.83		10.34-9.95	10.3
FA2	0.42± 0.15	---	
9.3-9.12			9.4
FA1	0.57± 0.15	AC3	
8.95-7.9		9.08-7.56	8.1

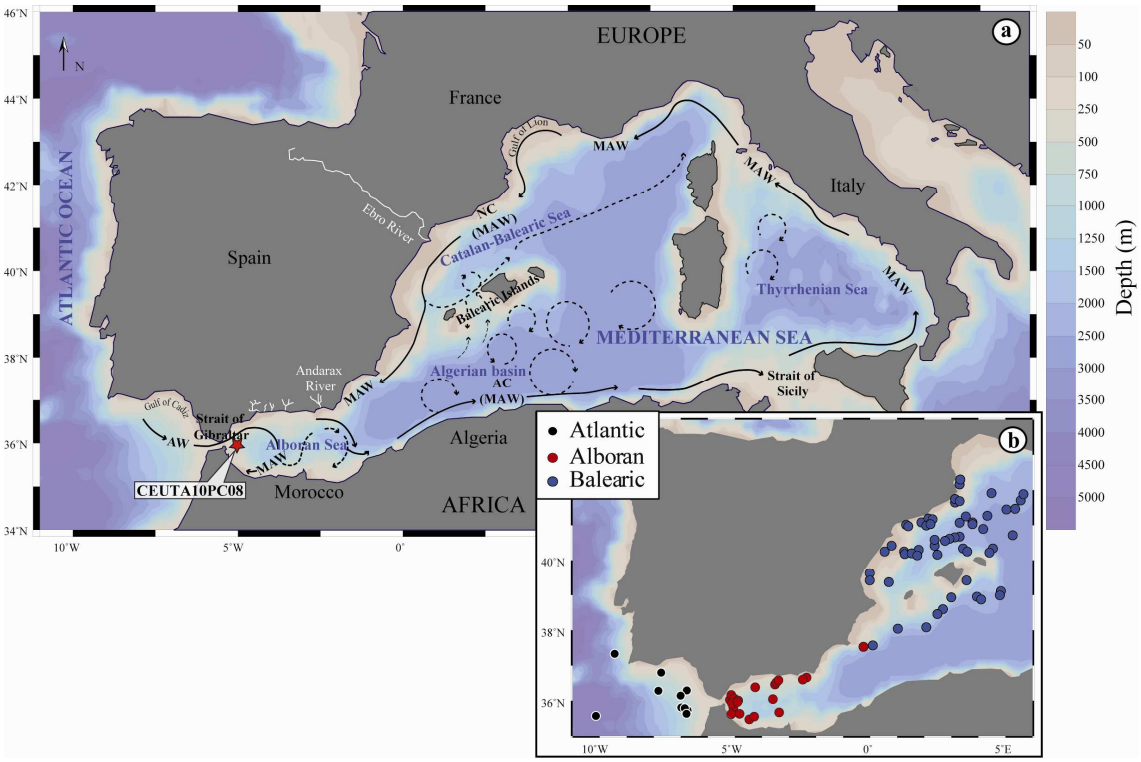

Figure 1. Maps of the study area. a) Location of the CEUTA10PC08 core (red star). Black arrows trace general surface circulation. Legend: AW: Atlantic Water. MAW: Modified Atlantic Water. AC: Algerian Current. NC: Northern Current. b) Location of the 88 core-top samples used for final calibrations. Maps generated with Ocean Data View software (Schlitzer, 2014).

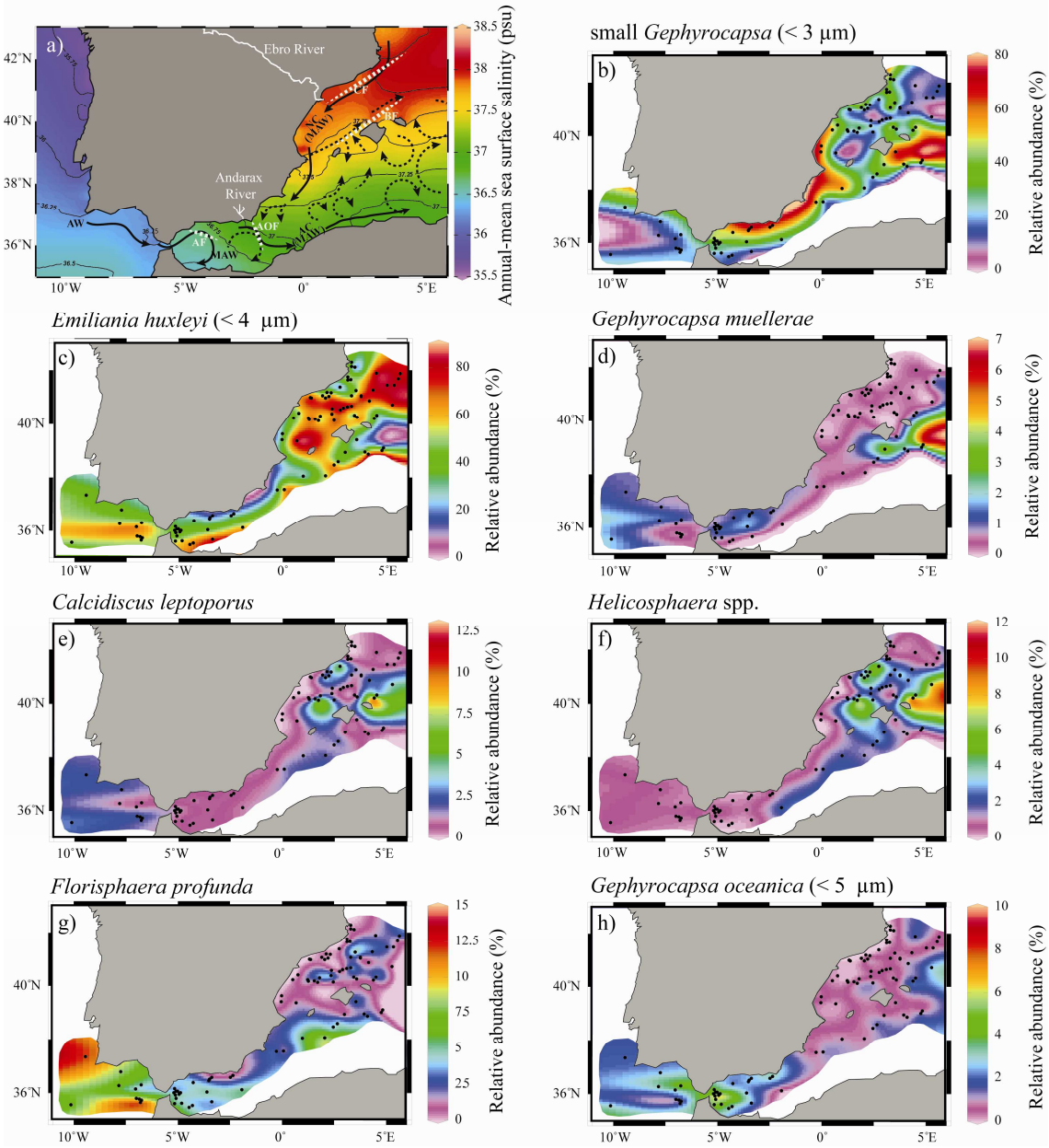

Figure 2. Geographical distribution of the main coccolithophore taxa. a) Annual-mean salinity at 10 m depth and surface circulation patterns in the study area: permanent trajectories (black arrows) and semi-permanent meso-scale features (dashed arrows). Legend: AF: Alboran Front; AOF: Almería-Orán Front; CF: Catalan Front; BF: Balearic Front; AW: Atlantic Water; MAW: Modified Atlantic Water; AC: Argelian Current; NC: Northern Current. Distribution, according to their relative abundance (%), of: b) small *Gephyrocapsa* (< 3 µm); c) *E. huxleyi* (< 4 µm); d) *G. muellerae*; e) *C. leptoporus*; f) *Helicosphaera* spp.; g) *F. profunda*; h) *G. oceanica* (< 5 µm).

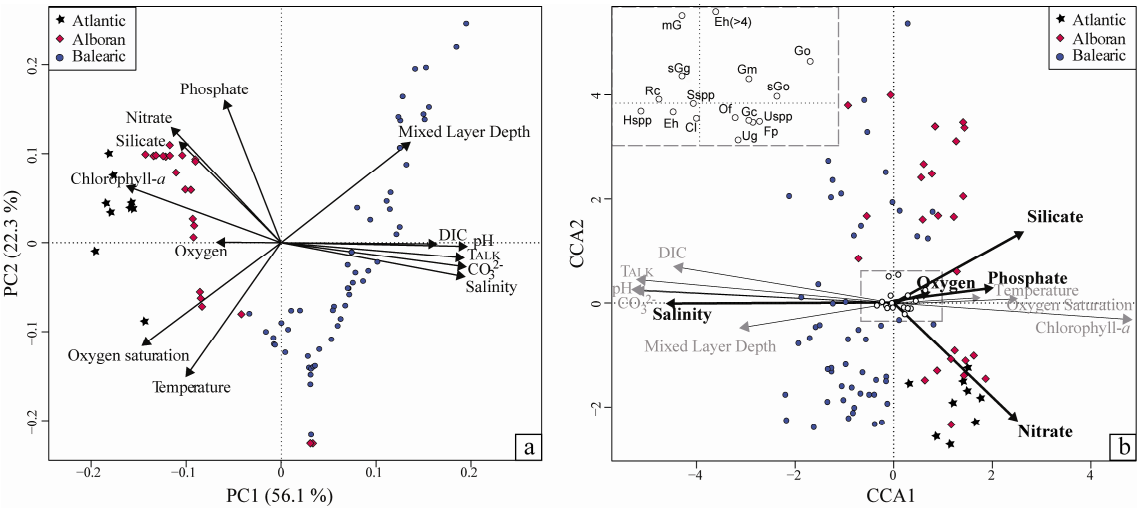

Figure 3. Multivariate analyses. a) PCA based on the thirteen initial environmental variables. b) CCA ordination plot with the site scores scaled by eigenvalues. The 88 sites are represented regarding their location in the Atlantic Ocean, Alboran Sea or Balearic Sea. Active and passive environmental vectors are represented by black and gray arrows, respectively. Scaling for the 16 taxa scores (open circles) is shown at the top left corner. mG: medium *Gephyrocapsa*; Eh(>4): *E. huxleyi* (> 4 µm); Eh: *E. huxleyi*; sGg: small *Gephyrocapsa*; Gm: *G. muellerae*; Go: *G. oceanica*; sGo: small *G. oceanica*; Rc: *R. clavigera*; Sspp: *Syracosphaer*a spp.; Of: *O. fraglis*; Gc: *G.* cf. *caribbeanica*; Hspp: *Helicosphaera* spp.; Cl: *C. leptoporus*; Uspp: *Umbellosphaera* spp.; Ug: *Umbilicosphaera* spp.; Fp: *F. profunda.*

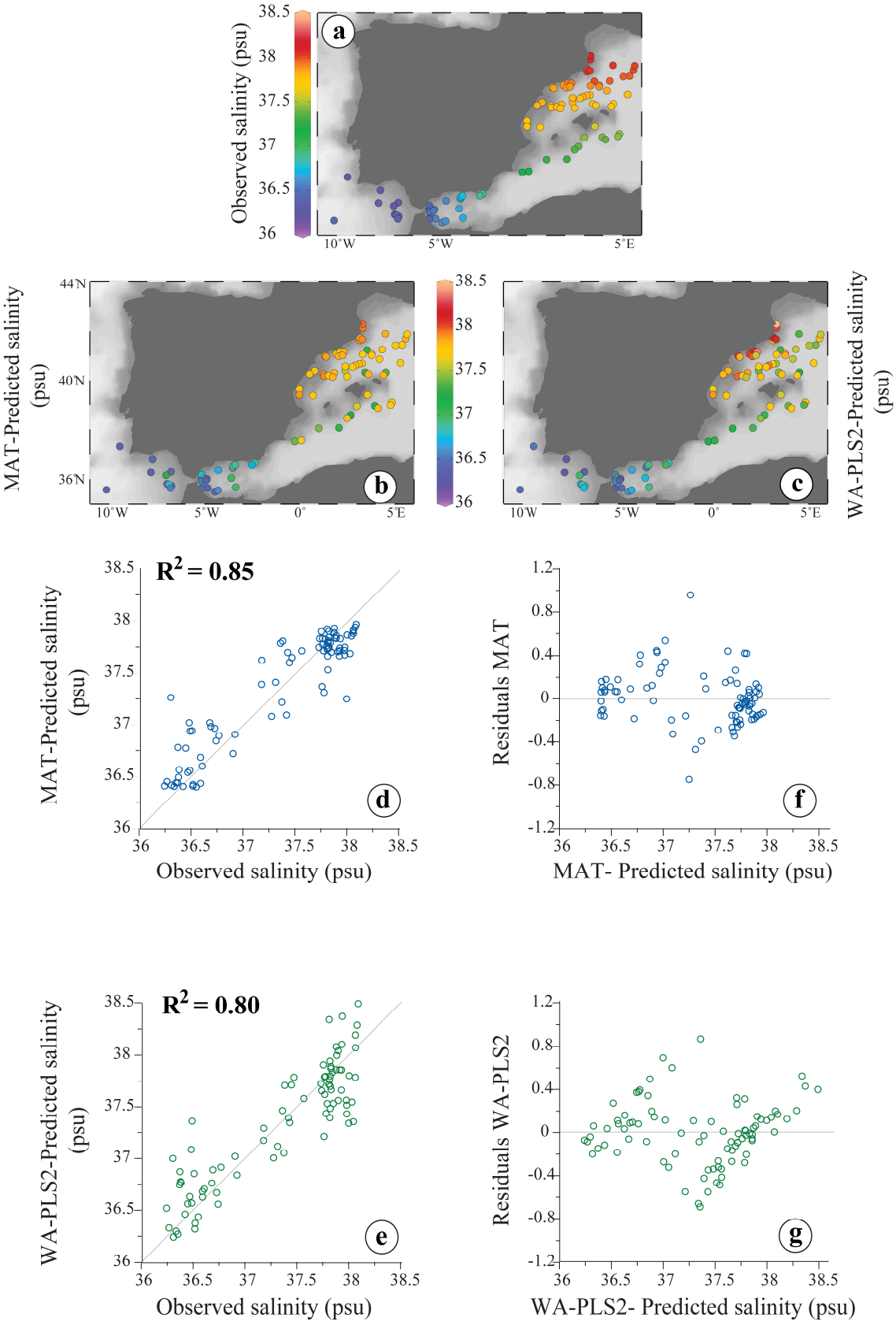

Figure 4. Diagnostic graphs of the models: a) Observed salinity values. b) MAT-predicted salinity values. c) WA-PLS2-predicted salinity values. d) Observed *vs* MAT-predicted salinity values. e) Observed *vs* WA-PLS2-predicted salinity values. f) MAT-predicted salinity values *vs* residuals. g) WA-PLS2-predicted salinity values *vs* residuals.

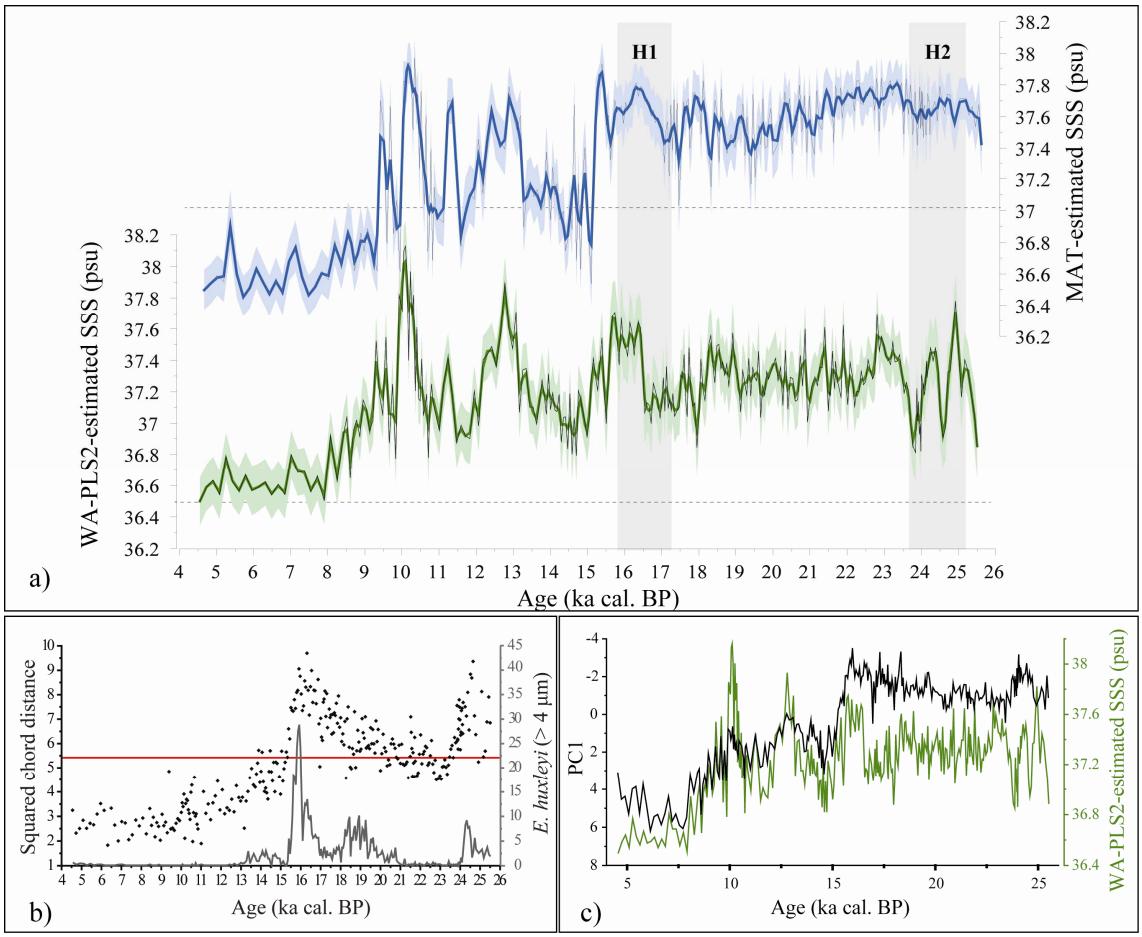

Figure 5. a) SSS reconstructions for the CEUTA10PC08 core derived from MAT (blue) and WA-PLS2 (green). The thin black lines represent the estimated values. The thick blue/green lines represent these original data fitted to a 3-point moving average smoothing spline. Pale blue/green shadows represent the error range, and dashed lines indicate current annual mean SSS in the Alboran Sea from the WOA13 (Zweng et al., 2013). b) Dissimilarity between modern and fossil assemblages (black dots) measured by squared chord distance (left axis) plotted *vs* age. The red line indicates the 10th percentile. Relative abundance of the species *E. huxleyi* (> 4 µm) (%; right axis). c) Profiles comparing the PC1$_{\mathbf{fossil}}$ (black line) and WA-PLS2-estimated SSS (green line).

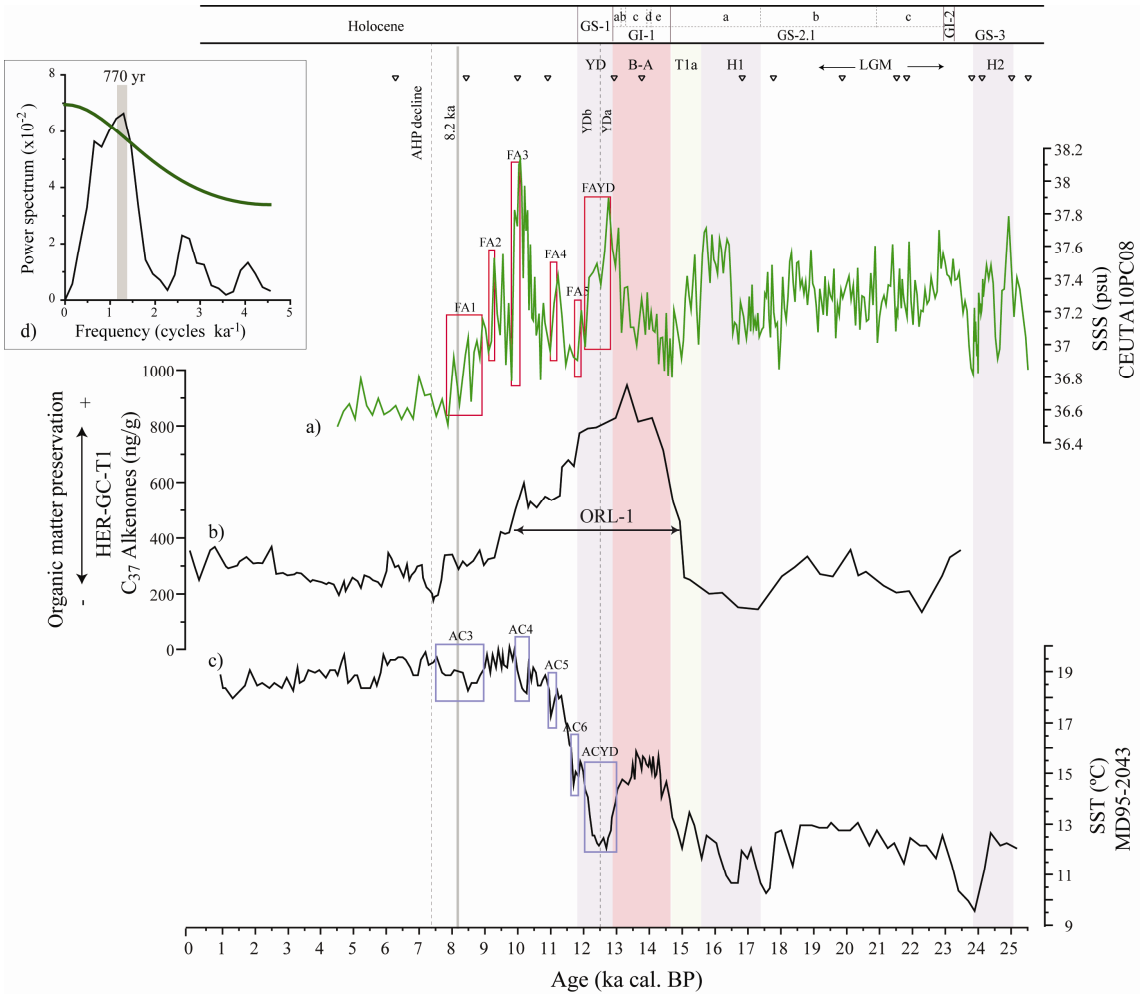

Figure 6. Paleoenvironmental records in the Alboran Sea: a) WA-PLS2-SSS reconstruction for CEUTA10PC08 core; age control points marked by triangles. b) C_{37} Alkenones from core HER-GC-T1 (Ausín et al., 2015). c) Alkenone-SST from core MD95-2043 (Cacho et al., 2001). Red boxes represent the Alboran cooling events (AC). d) REDFIT periodogram of the SSS reconstruction for the Holocene. The gray bar marks the only significant peak at the 95 % significance level (green line).